Terminal vs. Bridging Coordination of CO and NO Ligands after Decarbonylation of [W₂Cp₂(μ-PR₂)(CO)₃(NO)] Complexes (R = Ph, Cy). An Experimental and Computational Study†

M. Angeles Alvarez, M. Esther García, Daniel García-Vivó,* M. Teresa Rueda, Miguel A. Ruiz,* Adrián Toyos and M. Fernanda Vega.

Departamento de Química Orgánica e Inorgánica/IUQOEM, Universidad de Oviedo, E-33071 Oviedo, Spain.

Abstract

Compounds $[M_2Cp_2(\mu\text{-}PPh_2)(CO)_3(NO)]$ (M = Mo, W) were prepared by reacting the corresponding radicals $[M_2Cp_2(\mu\text{-}PPh_2)(CO)_4]$ with NO, and displayed a terminal, linear NO ligand arranged *cis* to the P-donor ligand (Mo–Mo = 3.1400(7) Å). The related PCy₂-bridged complex $[W_2Cp_2(\mu\text{-}PCy_2)(CO)_3(NO)]$ was prepared in a one-pot, three step procedure first involving deprotonation of the hydride complex $[W_2Cp_2(\mu\text{-}H)(\mu\text{-}PCy_2)(CO)_4]$ with K[BH(*sec*-Bu)₃], then oxidation of the resulting salt $K[W_2Cp_2(\mu\text{-}PCy_2)(CO)_4]$ with [FeCp₂]BF₄ at 243 K, and eventually by reacting the so-formed radical $[W_2Cp_2(\mu\text{-}PCy_2)(CO)_4]$ with NO. Photochemical decarbonylation of the Mo₂ complex gave intractable mixtures of products. In contrast, photolysis of the ditungsten complexes yielded the corresponding dicarbonyls $[W_2Cp_2(\mu\text{-}PR_2)(\mu\text{-}\kappa^1{:}\eta^2\text{-}CO)(CO)(NO)]$ (R = Ph, Cy) as major products, which were characterized spectroscopically. The latter reacted readily with P(OMe)₃ to give the corresponding derivatives $[W_2Cp_2(\mu\text{-}PR_2)(CO)_2(NO)\{P(OMe)_3\}]$, displaying a cisoid conformation of the P-donor ligands (P–W–P = 83.7(1)° when R = Cy). Density Functional Theory calculations on $[W_2Cp_2(\mu\text{-}PCy_2)(\mu\text{-}\kappa^1{:}\eta^2\text{-}CO)(CO)(NO)]$ and several potential isomers revealed that this electron-precise molecule (W–W = 3.121 Å) is almost isoenergetic with an unsaturated isomer having a $\mu\text{-}\kappa^1{:}\kappa^1\text{-}NO$ ligand (W–W = 2.677 Å) but their interconversion has a large kinetic barrier. It was concluded that formation of the $\kappa^1{:}\eta^2$-CO-bridged isomers in the photolytic experiment is favoured by the cisoid disposition of NO and PR₂ ligands at the parent tricarbonyls, which precludes the NO ligand from easily rearranging into a bridging position after decarbonylation. The above calculations also revealed that the CO ligand is much better suited than NO for the $\mu\text{-}\kappa^1{:}\eta^2$ coordination mode, since it can establish stronger *end-on* and *side-on* interactions with the dimetal centre.

Introduction

Decarbonylation of binuclear complexes is a classical strategy to prepare electronically and coordinatively unsaturated organometallic complexes, a class of molecules which usually will also display metal−metal multiple bonding. These species are of general interest because of their high reactivity under mild conditions towards a great variety of organic and inorganic molecules, whereby a very wide range of new products can be prepared in a selective way, many of them being not accessible through more conventional synthetic routes involving higher energy inputs, because of their decomposition under harsh conditions.[1-5] The ejection of a CO ligand from a binuclear complex generates a two-electron deficiency which, according to the 18-electron rule, will tend to be balanced by an increase in the intermetallic bond order by one unit. This is, however, usually accompanied by some rearrangement in the molecule to partially block the vacancy left after decarbonylation, particularly if other carbonyl ligands remain at the dimetal centre. Typical rearrangements include changes in the coordination of terminal carbonyls to bridging (μ-κ^1:κ^1) or semibridging modes, which do not modify the formal intermetallic bond order, as illustrated for the Mo_2 and W_2 complexes shown in Scheme 1.[6,7] Another possibility is that a remaining terminal carbonyl rearranges into the 4-electron donor, μ-κ^1:η^2 coordination mode, as found first for the dimanganese complex [Mn_2(μ-κ^1:η^2-CO)(CO)$_4$(μ-$Ph_2PCH_2PPh_2$)$_2$],[8] in which case the intermetallic bond order is not increased by the carbonyl loss (Scheme 1). Even in the latter event, however, the decarbonylated product remains highly reactive, since the bridging μ-κ^1:η^2-CO ligand readily reverts to the terminal mode upon addition of different reagents, as previously shown for the above Mn_2 complex,[9] and also for related [Mn_2(μ-κ^1:η^2-CO)(CO)$_5$L(μ-$Ph_2PCH_2PPh_2$)] species.[10]
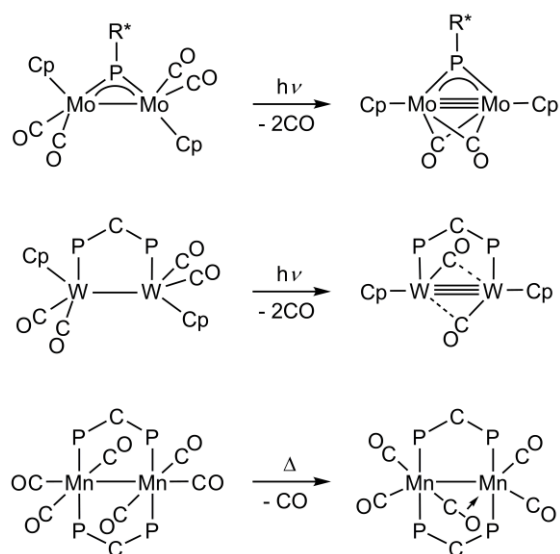
Scheme 1. Decarbonylation reactions of binuclear complexes (Cp = η^5-C_5H_5; R* = 2,4,6-$C_6H_2{}^tBu_3$; P–C–P = $Ph_2PCH_2PPh_2$)

Recently we became interested in the study of nitrosyl ligands at unsaturated dimetal centres based on the general idea that the inherent reactivity of these centres might facilitate transformations in the robust NO molecule that could be of interest in the context of the metal-catalyzed abatement of nitrogen oxides. For instance, we have shown that the unsaturated anions $[M_2Cp_2(\mu-PR_2)(\mu-CO)_2]^-$ (M = Mo, W; R = Ph, Cy) react at low temperatures with the cations $[M´(\eta^5-C_5H_4Me)(CO)_2(NO)]^+$ (M´ = Mn, Re) to give trinuclear oxo nitride derivatives which follow from a full N−O bond cleavage in the nitrosyl ligand.[11-12] Unfortunately, the number of unsaturated nitrosyl complexes available is quite limited, and their reactivity has been little explored so far due to synthetic problems or easy degradation toward mononuclear species. Thus, the synthesis of unsaturated nitrosyl complexes stabilized with respect to such a degradation remains a valuable goal in this context.[13] Following extensive work carried out previously by our group on the chemistry of phosphanyl-bridged unsaturated carbonyl complexes,[5] we then considered the possibility of preparing new unsaturated nitrosyl complexes through decarbonylation of suitable precursors properly stabilized with respect to degradation. The PPh$_2$-bridged tricarbonyl complex $[Mo_2Cp_2(\mu-PPh_2)(CO)_3(NO)]$ (**1**), a species reported some time ago in the context of our studies on the reactivity of the organometallic radical $[Mo_2Cp_2(\mu-PPh_2)(CO)_4]$,[14] seemed an excellent candidate for this purpose. In this paper we report full preparative and structural details of this complex, as well as those of the ditungsten analogues having PPh$_2$ and PCy$_2$ bridging ligands, and the results of our decarbonylation studies on all these tricarbonyl species. We were additionally interested in finding out whether the vacancy left by the loss of a carbonyl ligand in these substrates would induce any rearrangement in the remaining CO ligands, as shown in Scheme 1, or rather in the unique nitrosyl ligand at the place. Indeed, nitrosyl ligands are well known to bind dimetal centres in the same coordination modes as carbonyls do,[15] although the 5-electron donor, $\mu-\kappa^1:\eta^2$ coordination is an extremely rare mode for nitrosyls, with only two examples properly characterized so far.[16,17] As it will be shown below, our results indicate that both the CO and the NO ligands are able to properly stabilize the above substrates after decarbonylation, but adopting different bridging coordination modes, with CO being a more efficient ligand in the $\mu-\kappa^1:\eta^2$ mode, compared to the $\mu-\kappa^1:\kappa^1$ mode, whereas the reverse holds for NO.

Results and discussion

Synthesis of tricarbonyl nitrosyl complexes 1 and 2

We have previously shown that the nitrosyl complex **1** is obtained in good yield through the reaction of the paramagnetic complex $[Mo_2Cp_2(\mu-PPh_2)(CO)_4]$ with NO.[14] We have now found that the related ditungsten radical $[W_2Cp_2(\mu-PPh_2)(CO)_4]$[18] also reacts with

NO readily at 263 K to give the corresponding nitrosyl derivative [$W_2Cp_2(\mu$-$PPh_2)(CO)_3(NO)$] (**2a**) in good yield (Scheme 2).
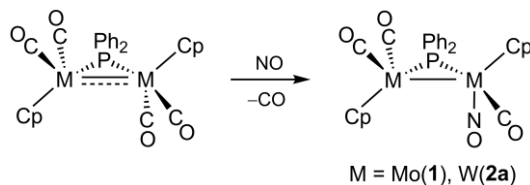
Scheme 2. Preparation of PPh$_2$-bridged nitrosyl complexes

The paramagnetic complexes [$M_2Cp_2(\mu$-$PPh_2)(CO)_4$] used in the synthesis of compounds **1** and **2a** are prepared *via* a two-step procedure involving deprotonation of the corresponding hydrides [$M_2Cp_2(\mu$-H)(μ-$PPh_2)(CO)_4$], followed by oxidation of the resulting anions.[18] We have now used this sequence to produce the PCy$_2$-bridged analogue of **2a** in a one-pot, three-step procedure without isolation of the corresponding intermediate species (Scheme 3). Thus, the hydride complex [$W_2Cp_2(\mu$-H)(μ-$PCy_2)(CO)_4$] was first deprotonated with K[BH(*sec*-Bu)$_3$] in tetrahydrofuran to give a solution of K[$W_2Cp_2(\mu$-$PCy_2)(CO)_4$] having IR C–O stretches (see the Experimental Section) comparable to those previously reported for the anion [$W_2Cp_2(\mu$-$PPh_2)(CO)_4$]$^-$.[18] This anionic complex was then oxidized with [$FeCp_2$]BF$_4$ at 243 K to give a green solution of the paramagnetic complex [$W_2Cp_2(\mu$-$PCy_2)(CO)_4$], which turned out to be quite unstable, and no attempts to isolate it were made. This NMR-silent product displayed C–O stretching bands at frequencies some 10 cm^{-1} below the corresponding positions for the analogous PPh$_2$-bridged complex as expected, but their number was doubled (six, rather than three bands; see the Experimental Section), which suggests the presence of conformers in solution, though this was not investigated. Reaction of this paramagnetic complex with nitric oxide (0.2% in N$_2$) at room temperature finally gave complex [$W_2Cp_2(\mu$-$PCy_2)(CO)_3(NO)$] (**2b**) as the major product, which could be isolated with an overall 87% yield after chromatographic workup.
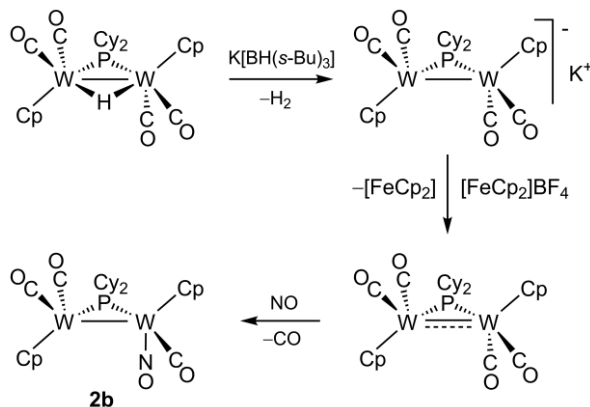
Scheme 3. Preparation of the PCy$_2$-bridged nitrosyl complex **2b**

Structural characterization of tricarbonyl nitrosyl complexes

The molecule of the dimolybdenum complex **1** in the crystal is built up from $MoCp(CO)_2$ and $MoCp(CO)(NO)$ fragments connected via a bridging PPh_2 ligand, with a transoid disposition of the Cp rings relative to the Mo_2P plane (Figure 1 and Table 1). The nitrosyl ligand adopts a conventional 3-electron donor, linear coordination mode (Mo−N = 1.794(6) Å; Mo−N−O = 178.4(5)°), which yields an overall 34-electron count for the complex. Therefore, a metal-metal single bond should be formulated for this molecule according to the 18-electron rule, which is consistent with the intermetallic separation of 3.1400(7) Å. The latter is somewhat shorter than the values of ca. 3.25-3.29 Å found for the isoelectronic complexes $[M_2Cp_2(\mu\text{-H})(\mu\text{-PRR}')(CO)_4]$,[19] all of which bear a comparable arrangement of ligands, if we ignore the bridging hydride. Interestingly, the nitrosyl ligand in **1** specifically occupies a position *cis* to the P atom (P1−Mo2−N = 93.9(2)°), while the CO ligand attached to the same metal centre is transoid to phosphorus (P1−Mo2−C3 = 111.8(2)°) and leaning over the intermetallic bond (Mo1−Mo2−C3 = 63.7(2)°). This particular stereochemistry is relevant to the decarbonylation reactions of these molecules, a matter to be discussed later on.
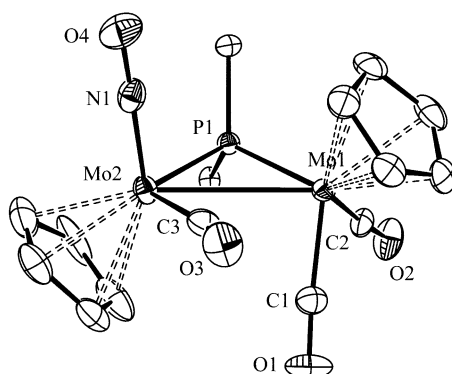

Fig. 1. ORTEP diagram (30% probability) of compound **1**, with H atoms and Ph rings (except their C[1] atoms) omitted for clarity.

Table 1. Selected bond lengths (Å) and angles (°) for compound **1**

Mo1−Mo2	3.1400(7)	Mo1−P1−Mo2	81.11(5)
Mo1−P1	2.387(1)	P1−Mo1−C1	108.9(2)
Mo2−P1	2.442(1)	P1−Mo1−C2	82.2(2)
Mo1−C1	1.951(7)	P1−Mo2−C3	111.8(2)
Mo1−C2	1.919(7)	P1−Mo2−N1	93.9(2)
Mo2−C3	1.984(7)	C1−Mo1−C2	79.0(3)
Mo2−N1	1.794(6)	N1−Mo2−C3	88.2(3)

Spectroscopic data in solution for compounds **1** and **2** (Table 2 and Experimental Section) are similar to each other and consistent with the solid-state structure of **1** discussed above. They all show a similar pattern for the X−O stretches, with three C−O stretching bands corresponding to terminal carbonyls and a N−O stretch at around 1620 cm^{-1} corresponding to the terminal nitrosyl. The relative frequencies of these bands (**1** >

2a > **2b**) follow the expected order derived from changes in metals and ligands (Mo > W and PPh$_2$ > PCy$_2$). Moreover, the ^{13}C NMR spectra for compounds **1** and **2a** indicate that the spatial arrangement of carbonyls found in the crystal (two carbonyls *trans* to P and one carbonyl *cis* to it) is preserved in solution, since in each case they show two carbonyl resonances with negligible P-C coupling (0-3 Hz), and just one resonance with a significant P-C coupling (ca. 20 Hz).[20] Finally we note that all these compounds display relatively deshielded ^{31}P NMR resonances, as expected for phosphanyl ligands bridging metal-metal bonded centres,[21] while the relative values of the corresponding spectroscopic parameters (δ_P, J_{PW}) are as expected.

Table 2. Selected IR,[a] and ^{31}P{^{1}H} data[b] for new compounds.

Compound	ν(CO)	ν(NO)	δ(P) [J_{PW}] (J_{PP})
[Mo$_2$Cp$_2$(μ-PPh$_2$)(CO)$_3$(NO)] (**1**)	1944 (vs), 1898 (s), 1853 (m)	1637 (m)	193.2
[W$_2$Cp$_2$(μ-PPh$_2$)(CO)$_3$(NO)] (**2a**)	1935 (vs), 1892 (s), 1839 (m)	1618 (m)	129.9 [328, 269]
[W$_2$Cp$_2$(μ-PCy$_2$)(CO)$_3$(NO)] (**2b**)	1926 (vs), 1881 (s), 1828 (m)	1610 (m)	149.0 [303, 254]
[W$_2$Cp$_2$(μ-PPh$_2$)(μ-κ^1:η^2-CO)(CO)(NO)] (**3a**)	1864 (vs), 1557 (m)[c]	1593 (s)[c]	145.5 [352, 288][d]
[W$_2$Cp$_2$(μ-PCy$_2$)(μ-κ^1:η^2-CO)(CO)(NO)] (**3b**)	1849 (vs), 1551 (s)	1578 (s)	162.6 [326, 260]
[W$_2$Cp$_2$(μ-PPh$_2$)(CO)$_2$(NO){P(OMe)$_3$}] (**4a**)[e]	1893 (vs), 1798 (s)	1587 (m)	145.2 [258, 242] (53) 128.4 [571] (53)[d]
[W$_2$Cp$_2$(μ-PCy$_2$)(CO)$_2$(NO){P(OMe)$_3$}] (**4b**)	1882 (vs), 1781 (s)	1571 (m)	174.5 [227, 216] (51) 129.9 [536] (51)[d]

[a] Recorded in dichloromethane solution, with X−O stretching bands [ν(XO)] in cm^{-1} (X = C, N). [b] Recorded in CD$_2$Cl$_2$ solution at 121.49 MHz and 298 K unless otherwise stated, with chemical shifts (δ) in ppm and ^{31}P-^{183}W or ^{31}P-^{31}P couplings (J_{PW} or J_{PP}) in Hz. [c] In tetrahydrofuran solution. [d] In C$_6$D$_6$ solution. [e] A minor isomer (**B**, see text) was also obtained, characterized by ^{31}P{^{1}H} NMR resonances at 149.8 (d, J_{PP} = 26, μ-PPh$_2$) and 129.5 ppm (d, J_{PP} = 26, POMe).

Synthesis and structural characterization of complexes 3

The tricarbonyl complexes **1** and **2** are thermally stable and remained essentially unchanged in refluxing toluene solutions for a few hours. In contrast, these complexes are readily decarbonylated upon irradiation with visible-UV light in tetrahydrofuran or toluene solutions at 288 K. The photolysis of the dimolybdenum complex **1** proceeded with very low selectivity to give a mixture of unstable products that could not be isolated nor properly characterized. In contrast, the photolysis of the ditungsten complexes **2a,b** proceeded smoothly with loss of a CO ligand to give the corresponding dicarbonyl derivatives [W$_2$Cp$_2$(μ-PR$_2$)(μ-κ^1:η^2-CO)(CO)(NO)] (R = Ph(**3a**), Cy(**3b**)) as major products (Scheme 4). The PPh$_2$-bridged complex **3a** was rather unstable and could not be isolated as a pure substance, although the crude product could be used for further reactions (see below). Fortunately, the PCy$_2$-bridged complex **3b** was somewhat more stable and could be isolated in the conventional way, although attempts to grow single crystals for an X-ray diffraction study were unsuccessful.
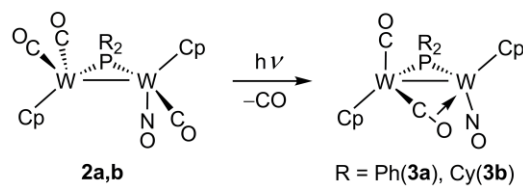
Scheme 4. Photolysis of complexes **2**

The IR spectrum of compounds **3** displays in each case a single band at around 1850 cm^{-1} which can be safely assigned to a terminal carbonyl, and two bands in the region 1550-1590 cm^{-1} corresponding to a terminal nitrosyl and the remaining carbonyl ligand. The very low frequency of the latter C–O stretch is not compatible with a conventional $\kappa^1:\kappa^1$ bridging mode, but rather suggests the presence of a 4-electron donor, μ-$\kappa^1:\eta^2$-CO ligand in this molecule. For comparison, the corresponding stretch in the thermally unstable complex [W$_2$Cp$_2$(μ-$\kappa^1:\eta^2$-CO)(CO)$_4$] was 1635 cm^{-1} (PVC film, 77 K),[22] and it was 1548 cm^{-1} for the structurally characterized diene complex [W$_2$Cp$_2$(μ-$\kappa^1:\eta^2$-CO)(CO)$_2$(η^4-CH$_2$CHCMeCHMe)].[23] Previous work on $\kappa^1:\eta^2$-CO-bridged dimanganese compounds has revealed that the ^{13}C NMR resonances for these ligands have chemical shifts comparable to those of terminal carbonyls.[10,24] This trend also seems to hold for tungsten compounds, because the carbonyl resonances for **3b** were found at 226.1 and 207.6 ppm. The latter resonance falls a bit below the usual range found for terminal carbonyls in this sort of complexes (cf. 240-222 ppm for **2a**), therefore we can safely assign it to the μ-$\kappa^1:\eta^2$-CO ligand of the complex. We finally note that complexes **3** display ^{31}P NMR resonances with chemical shifts comparable to those of their corresponding precursors, which is consistent with retention of the intermetallic bond order after decarbonylation, while the P–W couplings are a bit higher, as expected from the reduction in the overall number of ligands at the dimetal site. Spectroscopic differences between compounds **3a** and **3b** are as expected (as it was the case of the pair **2a/2b**) and deserve no further comments.
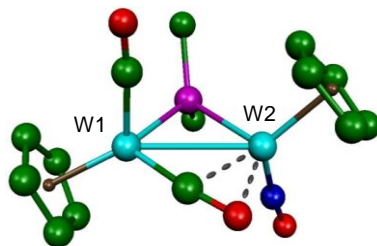

Fig. 2. DFT-optimized structure of compound **3b**, with H atoms and Cy groups (except their C^1 atoms) omitted for clarity. Selected bond lengths (Å): W1–W2 = 3.121; W1–P = 2.436; W1–COt = 1.943; W1–COb = 1.904; W2–P = 2.516; W2–N = 1.778; W2–COb = 2.242; W2–Ob = 2.211. Bond angles (°): W1–W2–NO = 104.4; W1–C–Ob = 168.9; W2–W1–COt = 89.3. C–O stretches, in cm^{-1} (% intensity): 1995 (90), 1630 (43); N–O: 1714 (100).

Density Functional Theory (DFT) calculations on **3b** were carried out in order to further support the proposed structure for compounds **3** and the spectroscopic analysis made above. As expected, the optimized structure of **3b** displays WCp(NO) and

WCp(CO) fragments in a relative transoid arrangement, bridged by a PCy$_2$ ligand in a slightly asymmetric way (W–P = 2.436 and 2.516 Å) and by a μ-κ^1:η^2-CO ligand (Figure 2). The latter is strongly *end-on* or σ-bound to the W1 atom, with a W–C length (1.904 Å) actually shorter than the corresponding length for the terminal ligand (1.943 Å), while the *side-on* or π-bonding interaction seems also quite strong, as judged from the relatively short W2–C and W2–O lengths of 2.242 and 2.211 Å respectively. There are only a few κ^1:η^2-CO-bridged Mo or W complexes structurally characterized to be used for comparative purposes.[23,25,26] In the above mentioned ditungsten diene complex, the corresponding M–C(σ), M–C(π) and M–O lengths were 1.90(1), 2.12(1) and 2.203(6) Å respectively, which we can viewed as comparable to the lengths computed for **3b**, after allowing for the usual overestimation of distances involving metal atoms in DFT calculations.[27] In contrast, the *side-on* interaction of the two κ^1:η^2-CO-ligands at the trimetal complex [MoW$_2$Cp$_2${μ-C(p-tol)}$_2$(μ-κ^1:η^2-CO)$_2$(CO)$_4$] seems to be substantially weaker, as judged from the corresponding Mo–C and Mo–O lengths of ca. 2.35 and 2.52 Å respectively, a circumstance that seems to correlate with the relatively high C–O stretch for these bridging ligands (1696 cm^{-1}).[26] In the case of **3b**, as a result of the strong *side-on* coordination of the bridging carbonyl, the molecule can be viewed as a genuine 34 electron-complex, therefore a metal-metal single bond should be formulated for this molecule according to the 18-electron rule, which is consistent with the computed intermetallic separation of 3.121 Å, a figure quite close to the length of 3.1400(7) Å experimentally determined for **1**. Finally, we note that the computed C–O and N–O stretches for **3b** (Figure 2) also were in good agreement with the experimental values measured in solution, after allowing for the usual ca. 5% overestimation in this sort of calculations.[28] This allows us to safely assign the less energetic band in each case (the band at ca. 1550 cm^{-1}) to the C–O stretch of the κ^1:η^2 bridging carbonyl present in compounds **3**.

Addition reactions of the dicarbonyl complexes 3

The *side-on* coordination of the bridging carbonyl ligand in compounds **3** is expectedly destroyed upon addition of simple donors such as CO or P(OMe)$_3$. These reactions take place readily at room temperature and involve the rearrangement of the bridging CO to a terminal position. Of course the addition of CO leads to the immediate regeneration of the parent tricarbonyls **2a,b**. Analogously, the reaction of the PCy$_2$-bridged complex **3b** with P(OMe)$_3$ leads selectively to the formation of the corresponding derivative [W$_2$Cp$_2$(μ-PCy$_2$)(CO)$_2$(NO){P(OMe)$_3$}] (**4b**), which is obtained as a single isomer (Chart 1). In contrast, the analogous reaction of **3a** yielded the corresponding product [W$_2$Cp$_2$(μ-PPh$_2$)(CO)$_2$(NO){P(OMe)$_3$}] (**4a**) as a mixture of two isomers **A** and **B** in a ratio of ca. 8:1, with the major isomer having the same structure as the unique isomer of **4b** (Chart 1).
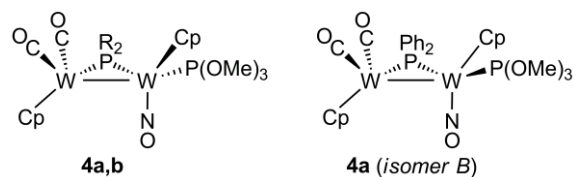
Chart 1

The molecular structure of the PCy$_2$-bridged complex **4b** was determined by a single-crystal X-ray diffraction study (Figure 3 and Table 3). The molecule, which is isoelectronic with compounds **1** and **2**, is built up now from WCp(CO)$_2$ and WCp(NO){P(OMe)$_3$} fragments connected *via* a bridging PCy$_2$ ligand, with a transoid disposition of the Cp rings relative to the W$_2$P plane and an essentially linear nitrosyl ligand, as found in **1** (W−N = 1.779(7) Å; W−N−O = 171.6(6)°). The intermetallic length of 3.0243(5) Å in this 34-electron complex, however, is ca. 0.12 Å shorter than the corresponding length in **1**, a difference that we attribute to the different conformations of the MCp(NO)L fragments in these two compounds. As noted above, the conformation of this fragment in **1** leaves the CO ligand *trans* to the P atom, but in compound **3b** the P(OMe)$_3$ ligand is placed *cis* to it (P−W−P = 83.7(1)°), while the NO ligand in both cases defines a P−M−N angle close to 95°. An analogous conformation has been previously found for the isoelectronic alkyl dinitrosyl complexes [Mo$_2$Cp$_2$(μ-PCy$_2$)R(CO)(NO)$_2$] (R = Me, CH$_2$Ph), which also display comparable Mo−Mo lengths of ca. 3.07-3.10 Å.[29]
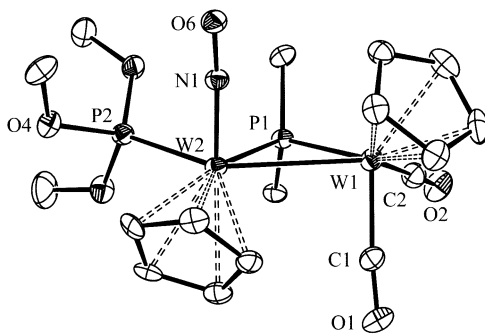

Fig. 3. ORTEP diagram (30% probability) of compound **4b**, with H atoms and Cy groups (except their C[1] atoms) omitted for clarity.

Table 3. Selected bond lengths (Å) and angles (°) for compound **4b**

W1−W2	3.0243(5)	W1−P1−W2	76.7(1)
W1−P1	2.405(2)	P1−W1−C1	100.5(3)
W2−P1	2.469(2)	P1−W1−C2	76.9(3)
W2−P2	2.385(2)	P1−W2−N1	95.7(2)
W1−C1	1.914(9)	P1−W2−P2	83.7(1)
W1−C2	1.97(1)	C1−W1−C2	81.0(4)
W2−N1	1.779(7)	N1−W2−P2	95.7(2)

Spectroscopic data in solution for compounds **4a,b** are consistent with the structure found in the solid state for **4b**. In particular, their IR spectra display two C−O stretches

with the intensities (very strong and strong, in order of decreasing frequencies) expected for $M(CO)_2$ oscillators defining a C–M–C angle just below 90° (81.0(4)° in the crystal).[30] The phosphanyl ligands in these compounds display ^{31}P chemical shifts comparable to those of the corresponding precursors **3**, but the one-bond P-W couplings are substantially lower, as expected from the increased number of ligands at the dimetal site, while the position and P-W couplings for the $P(OMe)_3$ ligands (δ_P ca. 130 ppm, $^1J_{PW}$ ca. 550 Hz) are not uncommon in this sort of molecule (cf. δ_P 134.7 ppm, $^1J_{PW}$ 512 Hz for $[W_2Cp_2(CO)_4\{\mu\text{-}(EtO)_2POP(OEt)_2\}]$.[31] The P-P couplings in compound **4b** and in the major isomer of **4a** are similar to each other and relatively large (51 and 53 Hz respectively), indicating comparable cisoid disposition of the PR_2 and $P(OMe)_3$ ligands in solution.[20] In contrast, the minor isomer of **4a** displays a much lower P-P coupling of 23 Hz, indicative of a larger P–W–P angle in this case, therefore consistent with a transoid relative positioning of the P-donor ligands for this minor isomer (Chart 1), which actually would correspond to the conformation exhibited by the tricarbonyl complexes **1** and **2**. Other spectroscopic features of compounds **3a,b** are as expected and deserve no further comment.

Terminal vs. bridging coordination of CO and NO ligands at the ditungsten complexes 3

As noted in the Introduction section, the nitrosyl ligand is able to act as a bridging group much in the same way as the carbonyl ligand does. In order to gain more insight about the thermodynamic preferences in our dimetal complexes we have computed, by using DFT methods (see the Experimental section and ESI), the structures and energies of different isomers of compound **3b** having either CO or NO ligands at the bridging site in either $\mu\text{-}\kappa^1{:}\kappa^1$ or $\mu\text{-}\kappa^1{:}\eta^2$ coordination modes (Figure 4), and we have also examined related isomers with a cisoid arrangement of the Cp ligands (see the ESI). The latter were systematically found to be less stable (by 10-25 kJ/mol) than the corresponding transoid isomers, which is a common feature in related group 6 metal complexes of type $[M_2Cp_2(\mu\text{-}X)(\mu\text{-}Y)L_2]$ (e.g. $[W_2Cp_2(\mu\text{-}PPh_2)_2L_2]$ complexes, with L = CO,[32] NO),[33] and they will not be further discussed. As expected, all structures having $\mu\text{-}\kappa^1{:}\eta^2$ bridging ligands (**3b**, **I1**, **I4**, and their *cis* congeners) display relatively large intermetallic separations of ca. 3.10 Å, consistent with the metal-metal single bond to be proposed for these 34-electron complexes. In contrast, all structures with $\mu\text{-}\kappa^1{:}\kappa^1$ ligands (**I2**, **I3**, and their *cis* congeners) correspond to 32-electron species, for which a metal-metal double bond should be formulated according to the 18-electron rule, which is consistent with the significantly shorter intermetallic separations of ca. 2.70 Å computed for all these isomers (i.e. 2.677 Å for **I3**, to be compared to 2.666(1) and 2.632(1) Å for *trans*-$[Mo_2Cp_2(\mu\text{-}PCy_2)(\mu\text{-}X)(CO)_2]$, with X = CPh, N=NHPh, respectively).[34,35] We note that the carbonyl-bridged structure **I2** was not a minimum when using the B3LYP

functional, unless forced to retain the μ-κ^1:κ^1 CO ligand (**I2*** in Figure 4, 91 kJ/mol above **3b**), but it was an authentic minimum (86 kJ/mol above **3b**) when using the ωB97XD functional and quasi-relativistic pseudopotentials (see the Experimental Section and the ESI). We interpret this difference as an indication that the structure **I2** actually is a quite shallow minimum in the potential energy surface of the system. On the other hand, since the nitrosyl-bridged structure **I3** was only 4 kJ/mol below **3b** at the B3LYP level, we also carried out further calculations on these two isomers and found that **3b** would be slightly more stable or less stable than **I3** depending on the functional used (see the ESI). From all this we conclude that isomers **3b** and **I3** have essentially identical energies and might co-exist in solution, a matter to be addressed below.
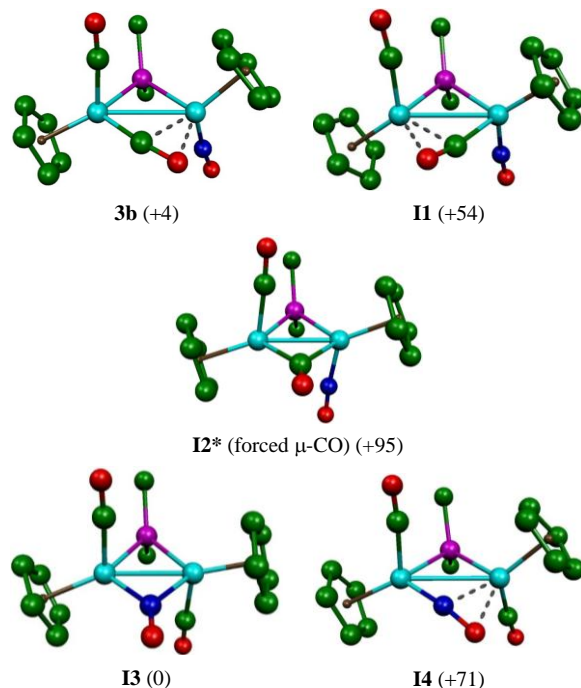

3b (+4)   **I1** (+54)

I2* (forced μ-CO) (+95)

I3 (0)   **I4** (+71)

Fig. 4. DFT-B3LYP computed structures for different isomers of compound **3b**, with H atoms and Cy groups (except their C[1] atoms) omitted, and their relative Gibbs free energies at 298 K (in kJ/mol) indicated between brackets. See the ESI for the corresponding *cis* isomers.

Other findings on the relative stability of the different isomers of **3b** are as follows: (a) The η^2 coordination of the bridging CO is clearly favoured when established with the NO-bearing metal fragment (**3b** 50 kJ/mol below **I1**); this is a sensible finding, because the formal electron contribution of the NO ligand is superior to that of a terminal CO (3 vs. 2 electrons), and then structure **3b** allows for a better balance of the intrinsic asymmetry of the μ-κ^1:η^2-CO coordination (π-bonding weaker than σ-bonding). (b) For the carbonyl ligand, the μ-κ^1:η^2 coordination provides a pronounced stabilization of some 90 kJ/mol to the system, when compared to its μ-κ^1:κ^1 coordination. In contrast, the reverse holds for the nitrosyl ligand, which yields a structure some 70 kJ/mol more stable when bound in the μ-κ^1:κ^1 mode. (c) As a

corollary of all the above findings we can also state that, in this system, the NO ligand is much more efficient than CO in the $\mu\text{-}\kappa^1\text{:}\kappa^1$ mode (**I3** 95 kJ/mol below **I2**).

To understand the pronounced differences between CO and NO ligands in the $\mu\text{-}\kappa^1\text{:}\eta^2$ coordination mode it is useful to analyze the different metal-ligand lengths computed for **3b** and **I4**. The W−C distance of 1.904 Å in **3b** is actually shorter than the corresponding value for its terminal carbonyl (1.943 Å), whereas the W−N length of 1.831 Å in **I4** is actually *longer* than the corresponding length for the terminal nitrosyl in **3b** (1.778 Å). This suggests that, in relative terms, the *end-on* interaction is much stronger for the carbonyl ligand in this coordination mode. Concerning the *side-on* interactions, we note that the W−C and W−N distances of 2.242 and 2.195 Å might be considered as comparable ones, if we allow for the 0.02 Å shorter covalent radius of N (compared to an *sp* C atom).[36] In contrast, the W−O distance is significantly shorter for **3b** (2.211 vs. 2.279 Å for **I4**), which is also reflected in a geometrical *attracto* effect in this case (W−C−O = 168.9°).[15] From this we conclude that the *side-on* interaction is stronger for the CO ligand, when compared to NO. In summary, in the $\mu\text{-}\kappa^1\text{:}\eta^2$ coordination mode the CO ligand is able to establish stronger *end-on* and *side-on* interactions with the metal atoms, when compared to NO, thus leading to a much more pronounced stabilization of the unsaturated dimetal centre. Since the steric properties of CO and NO are similar to each other, then this difference must be of electronic origin.

Reaction pathways following decarbonylation of compounds 2

As noticed in the preceding section, the computed energy for compound **3b** and that of its nitrosyl-bridged isomer **I3** are essentially identical and would allow for their co-existence in solution. However, the spectroscopic data available for compounds **3** clearly establish the presence of a single, $\kappa^1\text{:}\eta^2$-CO-bridged species in each case. Therefore it seems that compounds **3** are kinetic products. Initial photodecarbonylation at the WCp(CO)(NO) fragment would generate a coordination vacancy which would be rapidly blocked, with a minimum rearrangement, with the η^2-coordination of one of the carbonyl ligands of the WCp(CO)$_2$ fragment, to yield complexes **3** in a straightforward way. The alternative decarbonylation at the WCp(CO)$_2$ fragment of compounds **2** can be discarded as a productive photochemical event because this could only lead to quite unstable isomers of type **I1** or **I2**, but not to the more stable **I3**, since the nitrosyl ligand in the parent compounds **2** is positioned *cis* to the phosphanyl ligands, and therefore is unable to rearrange easily into a bridging position.

We have examined a possible rearrangement of the isolated product **3b** into its isoenergetic nitrosyl-bridged isomer **I3**. This would require the transfer of the strongly bound $\mu\text{-}\kappa^1\text{:}\eta^2$-CO ligand to the WCp(NO) fragment, while the nitrosyl ligand moves into a bridging position. This is likely a costly event, since we know from the chemistry and dynamics of this sort of ligands that they do not undergo scrambling between metal

centers.[10,24] Moreover, such a rearrangement would naturally yield isomer *cis*-**I3**, therefore it would need to be followed by a *cis* to *trans* rearrangement of the latter intermediate (Figure 5). This last step is assumed to be a thermally accessible process, since we have previously shown that the phosphanyl-bridged complexes *cis*-[$M_2Cp_2(\mu$-$PPh_2)_2(CO)_2$] (which are isoelectronic with isomers **I3**) rearrange readily at room temperature to yield the corresponding isomers *trans* (M = Mo, W).[32]
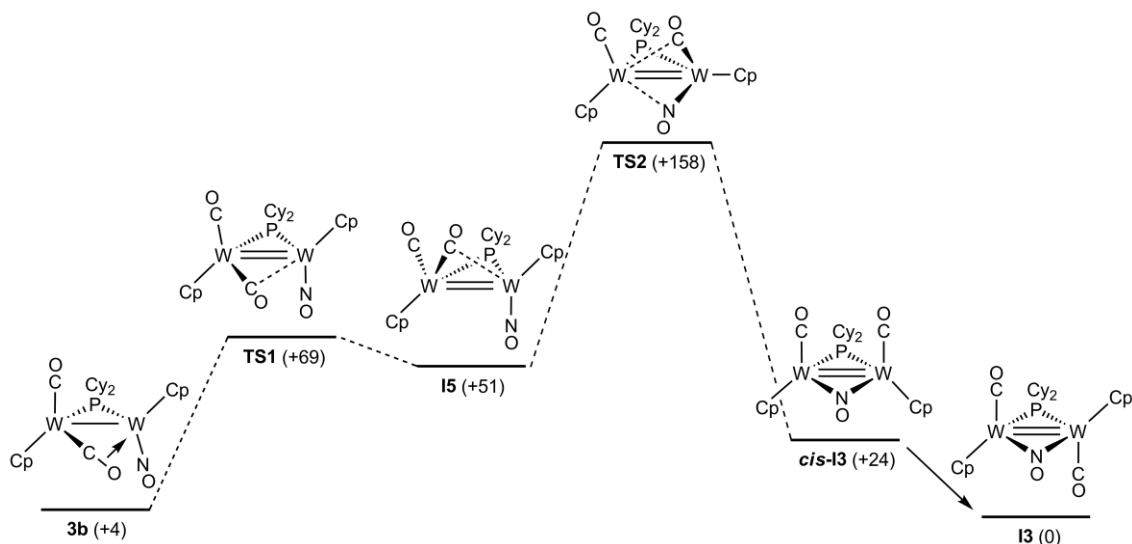

Fig. 5. DFT-B3LYP computed profile for a hypothetical isomerisation of **3b** into **I3**, with their relative Gibbs free energies at 298 K (in kJ/mol) indicated between brackets.

We have made calculations on a hypothetical **3b**/*cis*-**I3** isomerisation at the B3LYP level, and found that indeed it would involve a high kinetic barrier (Figure 5 and the ESI). Such a rearrangement would be initiated by a rotation of the WCp(CO)$_2$ fragment that destroys the *side-on* interaction of the bridging carbonyl, which then moves above the W$_2$P plane into a loosely semibridging position, yielding an unsaturated intermediate **I5** (W−W = 2.733 Å) placed 47 kJ/mol above **3b**. The required rearrangement is quite modest, and the corresponding transition state **TS1** is only a bit higher in energy than **I5** (65 kJ/mol above **5b**). This would be followed by a more complex rearrangement that involves the transfer of the semibridging carbonyl to the second metal atom, while the NO ligand moves into a bridging position and the Cp ligand flips into a cisoid positioning with respect to the other Cp ligand, this eventually yielding isomer *cis*-**I3**. The corresponding transition state **TS2** has semibridging CO and NO ligands and it is also unsaturated (W−W = 2.886 Å). It is placed 154 kJ/mol above **3b** and therefore defines the overall kinetic barrier for the isomerisation **3b**/**I3**, which then cannot take place under ordinary thermal conditions. The energetic costs of the above rearrangements also explain the preferred formation of isomers **3** during photolysis of the tricarbonyls **2**, since the initial species generated after the photolytic decarbonylation of these complexes would likely have a structure quite close to that of

intermediate **I5**, which then would rapidly decay to the stable isomers **3** in an almost barrierless way, since **TS1** is placed only 18 kJ/mol above **I5**, while a rearrangement into the nitrosyl-bridged isomer **I3** cannot take place at room temperature, because the corresponding barrier would be quite high (**TS2** 107 kJ/mol above **I5**).

Conclusions

The photochemical decarbonylation of complexes [$M_2Cp_2(\mu\text{-}PR_2)(CO)_3(NO)$] only leads to relatively stable products for the ditungsten substrates, which display structures of formula [$W_2Cp_2(\mu\text{-}PR_2)(\mu\text{-}\kappa^1{:}\eta^2\text{-}CO)(CO)(NO)$] bearing an *end-on/side-on*-bound bridging carbonyl ligand. DFT calculations on the PCy_2-bridged system indicate that these electron-precise complexes have a thermodynamic stability comparable to that of their unsaturated isomers *trans*-[$W_2Cp_2(\mu\text{-}PR_2)(\mu\text{-}NO)(CO)_2$] having a $\mu\text{-}\kappa^1{:}\kappa^1\text{-}NO$ ligand, but the products actually isolated are kinetically favoured for two main reasons: (a) The *cis* arrangement of PR_2 and NO ligands at the parent substrates precludes the NO from easily rearranging into a bridging position just after decarbonylation, whereas rearrangement of a carbonyl into the $\kappa^1{:}\eta^2$ bridging mode almost is a barrierless process in these substrates; (b) A hypothetical rearrangement of the observed $\kappa^1{:}\eta^2$-CO-bridged complex into its almost isoenergetic $\kappa^1{:}\kappa^1$-NO-bridged isomer would require, *inter alia*, full cleavage of the strong *side on*-coordination of the carbonyl ligand and its transfer to the second metal atom, and both processes impose a large kinetic barrier to the overall isomerisation, estimated in some 160 kJ/mol. Finally, our calculations also indicate that, in relative terms, the CO ligand is much better suited than NO for the $\mu\text{-}\kappa^1{:}\eta^2$ coordination mode, since it can establish stronger *end-on* and *side-on* interactions with the dimetal centre, whereas the reverse seems to hold when considering the $\mu\text{-}\kappa^1{:}\kappa^1$ coordination mode.

Experimental section

General procedures and starting materials

All manipulations and reactions were carried out under an argon (99.995%) atmosphere using standard Schlenk techniques. All experiments were carried out using Schlenk tubes equipped with Young´s valves. Solvents were purified according to literature procedures and distilled prior to use.[37] Petroleum ether refers to that fraction distilling in the range 338-343 K. Compounds [$M_2Cp_2(\mu\text{-}PPh_2)(CO)_4$] (M = Mo, W),[14,18] [$W_2Cp_2(\mu\text{-}H)(\mu\text{-}PCy_2)(CO)_4$],[38] and [$FeCp_2$]$BF_4$,[39] were prepared as described previously, while all other reagents were obtained from the usual commercial suppliers and used as received, unless otherwise stated. Photochemical experiments were performed using jacketed quartz Schlenk tubes cooled by tap water (ca. 288 K). A 400 W medium-

pressure mercury lamp placed ca. 1 cm away from the Schlenk tube was used for these experiments. Chromatographic separations were carried out using jacketed columns cooled by tap water (ca. 288 K) or by a closed 2-propanol circuit, kept at the desired temperature with a cryostat. Commercial aluminium oxide (activity I, 70-290 mesh) was degassed under vacuum prior to use. The latter was mixed under argon with the appropriate amount of water to reach the activity desired. IR stretching frequencies were measured in solution and are referred to as ν (solvent) and are given in cm^{-1}. Nuclear magnetic resonance (NMR) spectra were routinely recorded at 290 K unless otherwise stated. Chemical shifts (δ) are given in ppm, relative to internal tetramethylsilane (^{1}H, ^{13}C), or external 85% aqueous H_3PO_4 (^{31}P), and coupling constants (J) are given in Hz.

Preparation of [Mo$_2$Cp$_2$(μ-PPh$_2$)(CO)$_3$(NO)] (1). Nitric oxide (5% in N$_2$) was gently bubbled through a dichloromethane solution (20 mL) of [Mo$_2$Cp$_2$(μ-PPh$_2$)(CO)$_4$] (0.060 g, 0.097 mmol) at 263 K, and the mixture was stirred for 5 min, then allowed to reach room temperature and further stirred for 10 min to give a red-orange solution. The solvent was then removed under vacuum, and the residue dissolved in a minimum dichloromethane and chromatographed on alumina (activity III) at 288 K. Elution with petroleum ether yielded a trace amount of the known complex [MoCp(CO)$_2$(NO)]. Elution with dichloromethane/petroleum ether (1/3) gave an orange fraction yielding, after removal of solvents, compound **1** as an orange microcrystalline solid (0.048 g, 80%). The crystals used in the X-ray diffraction study were grown from a concentrated toluene solution of the complex at 253 K. Anal. Calcd for C$_{25}$H$_{20}$NO$_4$PMo$_2$: C, 48.33; H, 3.24; N, 2.25. Found: C, 48.16; H, 3.05; N, 2.10. ^{1}H NMR (300.13 MHz, CD$_2$Cl$_2$): δ 7.85-6.70 (m, 10H, Ph), 5.22 (d, J_{HP} = 1, 5H, Cp), 5.00 (s, 5H, Cp). ^{13}C{^{1}H} NMR (100.63 MHz, CD$_2$Cl$_2$): δ 252.9 (s, MoCO), 242.4 (d, J_{PC} = 23, MoCO), 233.1 (s, MoCO), 145.3 [d, J_{PC} = 37, C^1(Ph)], 141.4 [d, J_{PC} = 39, C^1(Ph)], 135.1 [d, J_{PC} = 10, C^2(Ph)], 132.2 [d, J_{PC} = 11, C^2(Ph)], 129.8, 128.7 [2s, C^4(Ph)], 128.8 [d, J_{PC} = 9, C^3(Ph)], 128.4 [d, J_{PC} = 10, C^3(Ph)], 96.9, 92.8 (2s, Cp).

Preparation of [W$_2$Cp$_2$(μ-PPh$_2$)(CO)$_3$(NO)] (2a). The procedure is identical to the one described for compound **1**, but using [W$_2$Cp$_2$(μ-PPh$_2$)(CO)$_4$] (0.080 g, 0.100 mmol) instead. Elution with petroleum ether yielded a trace amount of the known complex [WCp(CO)$_2$(NO)]. Elution with dichloromethane/petroleum ether (1/1) gave an orange fraction yielding, after removal of solvents, compound **2a** as an orange microcrystalline solid (0.057 g, 71%). Anal. Calcd for C$_{25}$H$_{20}$NO$_4$PW$_2$: C, 37.67; H, 2.53; N, 1.76. Found: C, 38.06; H, 2.55; N, 1.70. ^{1}H NMR (300.13 MHz, CD$_2$Cl$_2$): δ 7.75-6.80 (m, 10H, Ph), 5.29 (d, J_{HP} = 1, 5H, Cp), 5.10 (s, 5H, Cp). ^{13}C{^{1}H} NMR (75.48 MHz, CD$_2$Cl$_2$): δ 240.5 (d, J_{PC} = 3, WCO), 230.2 (d, J_{PC} = 19, WCO), 222.3 (d, J_{PC} = 3, WCO), 144.4 [d, J_{PC} = 47, C^1(Ph)], 140.8 [d, J_{PC} = 48, C^1(Ph)], 135.4. 132.9 [2d, J_{PC} =

10, C^2(Ph)], 129.8, 128.8 [2s, C^4(Ph)], 128.9, 128.5 [2d, J_{PC} = 10, C^3(Ph)], 95.3, 91.3 (2s, Cp).

Preparation of [W$_2$Cp$_2$(μ-PCy$_2$)(CO)$_3$(NO)] (2b). A tetrahydrofuran solution of K[BH(*sec*-Bu)$_3$] (0.56 mL of a 1M solution, 0.56 mmol) was added to a tetrahydrofuran solution (40 mL) of [W$_2$Cp$_2$(μ-H)(μ-PCy$_2$)(CO)$_4$] (0.230 g, 0.285 mmol), and the mixture was stirred at room temperature for 3.5 h to give an orange solution of K[W$_2$Cp$_2$(μ-PCy$_2$)(CO)$_4$] (νCO) = 1873 (m), 1838 (vs), 1777 (s), 1746 (w)). The solvent was then removed under vacuum and the residue was washed with petroleum ether (4 x 5 mL) and then dried under vacuum. Tetrahydrofuran (30 mL) was then added to this product and the solution was cooled at 243 K, then stirred with [FeCp$_2$]BF$_4$ (0.153 g, 0.56 mmol) for 45 min to give a green solution of the paramagnetic complex [W$_2$Cp$_2$(μ-PCy$_2$)(CO)$_4$] (νCO) = 1941 (sh, w), 1933 (w), 1899 (vs), 1881 (m), 1851 (s), 1836 (m)). Then nitric oxide (0.2% in N$_2$) was gently bubbled through this solution for 50 min to give an orange solution. After removal of the solvent, the residue was extracted with dichloromethane/petroleum ether (1/4) and the extracts chromatographed on alumina (activity IV) at 288 K. Elution with dichloromethane/petroleum ether (1/3) gave an orange fraction yielding, after removal of solvents, compound **2b** as an orange microcrystalline solid (0.200 g, 87%). Anal. Calcd for C$_{25}$H$_{32}$NO$_4$PW$_2$: C, 37.11; H, 3.99; N, 1.73. Found: C, 36.85; H, 3.71; N, 1.53. ^{1}H NMR (300.13 MHz, CD$_2$Cl$_2$): δ 5.61, 5.28 (2s, 2 x 5H, Cp), 2.10-1.00 (m, 22H, Cy).

Preparation of [W$_2$Cp$_2$(μ-PPh$_2$)(μ-κ^1:η^2-CO)(CO)(NO)] (3a). A tetrahydrofuran solution (15 mL) of compound **2a** (0.015 g, 0.038 mmol) was irradiated with visible-UV light at 288 K for 15 min, while gently bubbling N$_2$ (99.9999%) through the mixture, to give a brown solution which was filtered. Removal of solvent from the filtrate and washing of the residue with petroleum ether (2 x 3 mL) gave a brown solid containing compound **3a** as the major product, along with other uncharacterized species. Attempts to further purify this product led to its progressive decomposition. ^{1}H NMR (300.13 MHz, C$_6$D$_6$): δ 8.00-6.80 (m, 10H, Ph), 5.00, 4.77 (2d, J_{HP} = 1, 2 x 5H, Cp).

Preparation of [W$_2$Cp$_2$(μ-PCy$_2$)(μ-κ^1:η^2-CO)(CO)(NO)] (3b). A toluene solution (15 mL) of compound **2b** (0.080 g, 0.099 mmol) was irradiated with visible-UV light at 288 K for 20 min, while gently bubbling N$_2$ (99.9999%) through the mixture, to give a brown solution which was filtered. After removal of the solvent, the residue was extracted with dichloromethane/petroleum ether (1/2) and the extracts were chromatographed on alumina (activity IV) at 253 K. Elution with the same solvent mixture gave two minor orange fractions containing small amounts (less than 0.005 g) of compounds **2b** and [W$_2$Cp$_2$(μ-H)(μ-PCy$_2$)(CO)$_4$], respectively. Elution with neat dichloromethane gave a major yellow fraction yielding, after removal of solvents,

compound **3b** as a yellow solid (0.025 g, 32%). Anal. Calcd for $C_{24}H_{32}NO_3PW_2$: C, 36.90; H, 4.13; N, 1.79. Found: C, 36.65; H, 3.70; N, 1.58. ^{1}H NMR (300.13 MHz, CD_2Cl_2): δ 5.88, 5.48 (2s, 2 x 5H, Cp), 2.50-1.00 (m, 22H, Cy). $^{13}C\{^1H\}$ NMR (75.46 MHz, CD_2Cl_2): δ 226.1 (d, J_{CP} = 2, WCO), 207.6 (s, μ-κ^1:η^2-CO), 99.7, 87.5 (2s, Cp), 54.8 [d, J_{CP} = 19, C^1(Cy)], 54.0 [d, J_{CP} = 20, C^1(Cy)], 39.3 [s, C^2(Cy)], 35.6 [d, J_{CP} = 4, C^2(Cy)], 34.8 [d, J_{CP} = 6, C^2(Cy)], 34.6 [d, J_{CP} = 3, C^2(Cy)], 29.4 [d, J_{CP} = 13, C^3(Cy)], 29.0, 28.6 [2d, J_{CP} = 12, C^3(Cy)], 28.6 [d, J_{CP} = 9, C^3(Cy)], 26.7, 26.6 [2s, C^4(Cy)].

Preparation of [W$_2$Cp$_2$(μ-PPh$_2$)(CO)$_2$(NO){P(OMe)$_3$}] (4a). Neat P(OMe)$_3$ (20 μL, 0.170 mmol) was added to a tetrahydrofuran solution (10 mL) of the crude compound **3a** prepared from 0.030 g of compound **2a** (0.038 mmol) as described above, and the mixture was stirred at room temperature for 20 min to give a brown solution. After removal of the solvent, the residue was extracted with dichloromethane/petroleum ether (1/2) and the extracts were chromatographed on alumina (activity IV) at 288 K. Elution with neat dichloromethane gave an orange fraction yielding, after removal of solvents, compound **4a** as an orange solid (0.015 g, 44%). This product was shown by NMR to be a mixture of two isomers (**A** and **B**) in a ratio **A/B** = 8 (see text). Anal. Calcd for $C_{27}H_{29}NO_6P_2W_2$: C, 36.31; H, 3.27; N, 1.57. Found: C, 36.10; H, 2.95; N, 1.43. *Spectroscopic data for isomer A*: ^{1}H NMR (300.13 MHz, C_6D_6): δ 7.90-6.90 (m, 10H, Ph), 5.42 (d, J_{HP} = 1, 5H, Cp), 5.12 (s, 5H, Cp), 2.88 (d, J_{HP} = 11, 9H, OMe). *Spectroscopic data for isomer B*: ^{1}H NMR (300.13 MHz, C_6D_6): δ 5.04, 4.92 (2s, 2 x 5H, Cp), 3.30 (d, J_{HP} = 11, 9H, OMe).

Preparation of [W$_2$Cp$_2$(μ-PCy$_2$)(CO)$_2$(NO){P(OMe)$_3$}] (4b). Neat P(OMe)$_3$ (20 μL, 0.170 mmol) was added to a toluene solution (15 mL) of the crude compound **3b** prepared from 0.030 g of compound **2b** (0.037 mmol) as described above, and the mixture was stirred at room temperature for 20 min to give a brown solution. After removal of the solvent, the residue was extracted with dichloromethane/petroleum ether (1/1) and the extracts were chromatographed on alumina (activity IV) at 288 K. Elution with dichloromethane/petroleum ether (2/1) gave an orange fraction yielding, after removal of solvents, compound **4b** as an orange solid (0.020 g, 60%). The crystals used in the X-ray diffraction study were grown through the slow diffusion of a layer of petroleum ether into a concentrated toluene solution of the complex at 253 K. Anal. Calcd for $C_{27}H_{41}NO_6P_2W_2$: C, 35.82; H, 4.57; N, 1.55. Found: C, 35.58; H, 4.35; N, 1.40. ^{1}H NMR (300.13 MHz, C_6D_6): δ 5.41 (d, J_{HP} = 1, 5H, Cp), 5.38 (s, 5H, Cp), 3.19 (d, J_{HP} = 11, 9H, OMe), 3.00-0.70 (m, 22H, Cy).

X-ray structure determination of compound 1

Data collection was performed at 291 K on a Phillips PW1100 single crystal diffractometer, using graphite-monochromated Mo-Kα radiation. Two standard reflections were monitored periodically and showed no decay. Corrections were made

for Lorenz and polarization effects, and empirical absorption (Difabs)[40] and extinction corrections were applied. Computations were performed by using CRYSTALS,[41] and atomic form factors for neutral Mo, P, O, N, C and H were taken from ref. 42. The structure was solved by direct methods (SHELXS)[43] and successive Fourier maps. All non-hydrogen atoms were refined anisotropically. All hydrogen atoms could be found on difference maps, but their positions were not refined and they were given an overall isotropic parameter. Full matrix least squares refinements were carried out by minimizing the function $\Sigma(F_o-|F_c|)^2$ where F_o and F_c are the observed and calculated structure factors.

<div align="center">Table 4. Crystal data for new compounds.</div>

	1	4b
mol formula	$C_{25}H_{20}Mo_2NO_4P$	$C_{27}H_{41}NO_6P_2W_2$
mol wt	621.27	905.23
cryst syst	monoclinic	monoclinic
space group	$P\,2_1/a$	$P\,2_1/c$
radiation (λ, Å)	0.71069	1.54184
a, Å	17.296(3)	12.0125(3)
b, Å	16.028(5)	15.8531(5)
c, Å	8.760(2)	18.6734(6)
α, deg	90	90
β, deg	101.46(2)	93.514(3)
γ, deg	90	90
V, Å^3	2380(2)	3549.4(2)
Z	4	4
calcd density, g cm^{-3}	1.73	1.694
absorp coeff, mm^{-1}	1.13	12.939
temperature, K	291(1)	100.0(1)
θ range (deg)	1.00-25.00	3.66-69.29
index ranges (h, k, l)	−20, 20; 0, 19; 0, 10	−14, 12; −19, 13; −16, 22
no. of indep reflns (R_{int})	4207 (0.027)	6502 (0.028)
no. of reflns with $I > n\sigma(I)$	2522 (n = 3)	5907 (n = 2)
R indexes [data with $I > n\sigma(I)$]	$R_1 = 0.032$ $wR_2 = 0.033^a$	$R_1 = 0.0414$ $wR_2 = 0.1309^b$
GOF	1.038	0.832
no. of restraints/parameters	0 / 300	0 / 346
$\Delta\rho$(max., min.), eÅ^{-3}	0.40 / −0.40	1.20 /−1.27
CCDC deposition No	1547968	1547969

^{a} $R = \Sigma||F_o| - |F_c|| \,/\, \Sigma|F_o|$; $wR = [\Sigma(|F_o| - |F_c|)^2 \,/\, \Sigma|F_o|^2]^{1/2}$; ^{b} $R = \Sigma||F_o| - |F_c|| \,/\, \Sigma|F_o|$; $wR = [\Sigma w(|F_o|^2 - |F_c|^2)^2 \,/\, \Sigma w|F_o|^2]^{1/2}$; $w = 1/[\sigma^2(F_o^2) + (aP)^2 + bP]$ where $P = (F_o^2 + 2F_c^2)/3$; $a = 0.0884$, $b = 66.1530$.

X-ray structure determination of compound 4b

Data collection was performed at 100 K on an Oxford Diffraction Xcalibur Nova single crystal diffractometer, using Cu-K$_\alpha$ radiation. Images were collected at a 63 mm fixed crystal-detector distance, using the oscillation method, with 1° oscillation and variable exposure time per image (10-40 s). Data collection strategy was calculated with the program *CrysAlis Pro CCD*,[44] and data reduction and cell refinement was performed with the program *CrysAlis Pro RED*.[44] An empirical absorption correction was applied

using the SCALE3 ABSPACK algorithm as implemented in the latter program. Using the program suite WINGX,[45] the structure was solved by Patterson interpretation and phase expansion using SHELXL2016, and refined with full-matrix least squares on F^2 using SHELXL2016,[46] to give the residuals collected in Table 4. All non-hydrogen atoms were refined anisotropically, and all hydrogen atoms were geometrically placed and refined using a riding model. The complex crystallized with a highly disordered toluene molecule which could not be satisfactorily modelled; therefore, the SQUEEZE procedure,[47] as implemented in PLATON,[48] was used. Upon squeeze application and convergence, the strongest residual peak (1.20 eÅ^{-3}) was located near the W(1) atom.

Computational details

All DFT computations were carried out using the GAUSSIAN03 and GAUSSIAN09 packages,[49,50] in which the hybrid method B3LYP was used with the Becke three-parameter exchange functional[51] and the Lee-Yang-Parr correlation functional.[52] A pruned numerical integration grid (99, 590) was used for all the calculations *via* the keyword Int=Ultrafine. Effective core potentials and their associated double-ζ LANL2DZ basis set were used for the metal atoms.[53] The light elements (P, O, C, N and H) were described with the 6-31G* basis.[54] Geometry optimizations were performed under no symmetry restrictions, and frequency analyses were performed for all the stationary points to ensure that minimum structures with no imaginary frequencies were achieved. Molecular graphics and vibrational modes were visualized using the Molekel program.[55] Several DFT functionals were used to evaluate the energetic difference between isomers **3b** and **I3**, this including the standard generalized gradient approximation (GGA) functional BP86,[56] the hybrid meta-GGA functional ωB97XD containing empirical dispersion terms and also long-range corrections,[57] and the hybrid M06 functional designed to account for non-covalent attractions and dispersion via extensive parametrization using training sets including non-covalently bound complexes as well as TM energetics.[58] Also quasi-relativistic effective core potentials of the Stuttgart–Dresden type (SDD) and their associated basis set were used for the W atoms in some calculations to account for scalar relativistic effects expected to be important for heavy elements.[59]

Notes and references

Departamento de Química Orgánica e Inorgánica / IUQOEM, Universidad de Oviedo, E-33071 Oviedo, Spain. E-mail: garciavdaniel@uniovi.es (D. G. V.), mara@uniovi.es (M.A.R.)

1. F. A. Cotton and R. A. Walton, *Multiple Bonds between Metal Atoms, 2nd ed.*, Oxford University Press, Oxford, U. K., 1993, chapter 9.
2. M. D. Curtis, *Polyhedron,* 1987, **6**, 759.
3. M. J. Winter, *Adv. Organomet. Chem.,* 1989, **29**, 101.
4. J. P. Collman and R. Boulatov, *Angew. Chem. Int. Ed.* 2002, **41**, 3948.
5. D. García-Vivó, A. Ramos and M. A. Ruiz, *Coord. Chem. Rev.,* 2013, **257**, 2143.
6. (a) M. E. García, V. Riera, M. A. Ruiz, D. Sáez, H. Hamidov, J. C. Jeffery and T. Riis-Johannessen, *J. Am. Chem. Soc.,* 2003, **125**, 13044; (b) I. Amor, M. E. García, M. A. Ruiz, D. Sáez, H. Hamidov and J. C. Jeffery, *Organometallics,* 2006, **25**, 4857.
7. M. A. Alvarez, M. E. García, V. Riera, M. A. Ruiz, L. R. Falvello and C. Bois, *Organometallics,* 1997, **16**, 354.
8. (a) R. Colton and C. J. Commons, *Aust. J. Chem.,* 1975, **28**, 1663.
9. (a) A. L. Balch and L. S. Benner, *J. Organomet. Chem.,* 1977, **145**, 339; (b) H. C. Aspinall and A. J. Deeming, *J. Chem. Soc., Chem. Commun.* 1981, 724. (c) T. W. Turner, *Inorg. Chim. Acta,* 1982, **135**, L141.
10. X. Y. Liu, V. Riera, M. A. Ruiz and C. Bois, *Organometallics,* 2001, **20**, 3007.
11. M. E. García, D. García-Vivó, S. Melón, M. A. Ruiz, C. Graiff and A.Tiripicchio, *Inorg. Chem.,* 2009, **48**, 9282.
12. M. A. Alvarez, M. E. García, D. García-Vivó, M. A. Ruiz, A. Toyos and M. F. Vega, *Inorg. Chem.,* 2013, **52**, 3942.
13. M. A. Alvarez, M. E. García, D. García-Vivó, M. A. Ruiz and A.Toyos, *Dalton Trans.,* 2016, **45**, 13300, and references therein.
14. M. E. García, V. Riera, M. T. Rueda, M. A. Ruiz, M. Lanfranchi and A. Tiripicchio, *J. Am. Chem. Soc.,* 1999, **121**, 4060.
15. G. B. Ritcher-Addo and P. Legzdins, *Metal Nitrosyls*, Oxford University Press, Oxford, U. K., 1992.

16. (a) P. Legzdins, S. J. Rettig and J. E Veltheer, *J. Am. Chem. Soc.,* 1992, **114**, 6922; (b) P. Legzdins, S. J. Rettig, J. E. Veltheer, R. J. Batchelor and F. W. B. Einstein, *Organometallics,* 1993, **12**, 3575.

17. J. Ipaktschi, J. Mohseni-Ala, A. Dulmer, S. Steffens, C. Wittenburg and J. Heck, *Organometallics,* 2004, **23**, 4902.

18. C. M. Alvarez, M. E. García, M. T. Rueda, M. A. Ruiz, D. Sáez and N. G. Connelly, *Organometallics,* 2005, **24**, 650.

19. (a) C. M. Alvarez, M. A. Alvarez, M. E. García, D. García-Vivó, M. A. Ruiz, D. Sáez, L. R. Falvello, T. Soler and P. Herson, *Dalton Trans.,* 2004, 4168; (b) C. M. Alvarez, M. A. Alvarez, M. Alonso, M. E. García, M. T. Rueda, M. A. Ruiz and P. Herson, *Inorg. Chem.,* 2006, **45**, 9593.

20. A general trend established for $^2J_{XY}$ in complexes of the type $[MCpXYL_2]$ is that $|J_{cis}| > |J_{trans}|$. See, for instance, (a) C. J. Jameson, in *Phosphorus-31 NMR Spectroscopy in Stereochemical Analysis*, J. G. Verkade and L. D. Quin, Eds., VCH, Deerfield Beach, FL, 1987, Chapter 6; (b) B. Wrackmeyer and H. G. Alt, *J. Organomet. Chem.,* 1990, **399**, 125.

21. A. J. Carty, S. A. MacLaughlin and D. Nucciarone, in *Phosphorus-31 NMR Spectroscopy in Stereochemical Analysis*, J. G. Verkade and L. D. Quin, Eds., VCH, Deerfield Beach, FL, 1987, chapter 16.

22. R. H. Hooker and A. J. Rest, *J. Chem. Soc., Dalton Trans.,* 1990, 1221.

23. C. G. Kreiter, U. Kern, G. Wolmershäuser and G.Heckman, *Eur. J. Inorg. Chem.,* 1998, 127.

24. J. A. Marsella and K. G. Caulton, *Organometallics,* 1982, **1**, 274.

25. C. G. Kreiter, A. Würtz and P. Bell, *Chem. Ber.,* 1992, **125**, 377.

26. G. A. Carriedo, J. A. K. Howard, K. Marsden, F. G. A. Stone and P. Woodward, *J. Chem. Soc., Dalton Trans.,* 1984, 1589.

27. (a) C. J. Cramer, *Essentials of Computational Chemistry, 2nd Ed.*, Wiley, Chichester, UK, 2004; (b) W. Koch and M. C. Holthausen, *A Chemist´s Guide to Density Functional Theory, 2nd Ed.*, Wiley-VCH, Weinheim, 2002.

28. L. Yu, G. N. Srinivas and M. Schwartz, *J. Mol. Struct. (Theochem)*, 2003, **625**, 215.

29. M. A. Alvarez, M. E. García, M. E. Martínez, A. Ramos and M. A. Ruiz, *Organometallics,* 2009, **28**, 6293.

30. P. S. Braterman, *Metal Carbonyl Spectra*, Academic Press, London, U. K., 1975.

31. M. A. Alvarez, C. Alvarez, M. E. García, V. Riera, M. A. Ruiz and C. Bois, *Organometallics,* 1997, **16**, 2581.

32. M. A. Alvarez, M. E. García, M. E. Martinez, A. Ramos, M. A. Ruiz, D. Sáez and J. Vaissermann, *Inorg. Chem.,* 2006, **45**, 6965.

33. M. A. Alvarez, M. E. García, D. García-Vivó, S. Melón, M. A. Ruiz and A. Toyos, *Inorg. Chem.,* 2014, **53**, 4739.

34. M. A. Alvarez, M. E. García, D. García-Vivó, M. E. Martínez and M. A. Ruiz, *Organometallics,* 2011, **30**, 2189.

35. M. A. Alvarez, M. E. García, A. Ramos and M. A. Ruiz, *Organometallics,* 2007, **26**, 1461.

36. B. Cordero, V. Gómez, A. E. Platero-Prats, M. Revés, J. Echevarría, E. Cremades, F. Barragán and S. Alvarez, *Dalton Trans.,* 2008, 2832.

37. W. L. F. Armarego and C. Chai, *Purification of Laboratory Chemicals, 7th ed.*, Butterworth-Heinemann, Oxford, U. K, 2012.

38. M. E. García, V. Riera, M. A. Ruiz, M. T. Rueda and D. Sáez, *Organometallics,* 2002, **21**, 5515.

39. N. G. Connelly and W. E. Geiger, *Chem. Rev.,* 1996*,* **96***,* 877.

40. N. Walker and D. Stuart, *Acta Crytallogr., Sect. A*, 1983, **39**, 158.

41. D. J. Watkin, J. R. Carruthers and P. W. Betteridge, *Crystals User Guide*, Chemical Crystallography Laboratory, Oxford, U. K., 1988.

42. *International Tables for X-ray Crystallography, Vol. IV*, Kynoch Press, Birmingham, U.K., 1974.

43. G. M. Sheldrick, *SHELXS 86, Program for Crystal Structure Solution*, University of Göttingen, Göttingen, Germany, 1986.

44. *CrysAlis Pro*, Oxford Diffraction Limited, Ltd., Oxford, U. K., 2006.

45. L. J. Farrugia, *J. Appl. Crystallogr.,* 1999, **32**, 837.

46. (a) G. M. Sheldrick, *Acta Crystallogr., Sect. A,* 2008, **64**, 112; (b) G. M. Sheldrick, *Acta Crystallogr., Sect. C,* 2015, **71**, 5.

47. A. L. Spek, *Acta Crystallogr., Sect. C,* 2015, **71**, 9.

48. A. L. Spek, *PLATON, A Multipurpose Crystallographic Tool*, Utrecht University, Utrecht, The Netherlands, 2010.

49. M. J. Frisch, *et al.*, *Gaussian 03, Revision B.02*, Gaussian, Inc.: Wallingford, CT, 2004, see the ESI† for the complete reference.

50. M. J. Frisch, *et al.*, *Gaussian 09, Revision B.1*, Gaussian, Inc.: Wallingford, CT, 2009, see the ESI† for the complete reference.

51. A. D. Becke, *J. Chem. Phys.,* 1993, **98**, 5648.

52. C. Lee, W. Yang and R. G. Parr, *Phys. Rev. B,* 1988, **37**, 785.

53. P. J. Hay and W. R. Wadt, *J. Chem. Phys.,* 1985, **82**, 299.

54. (a) P. C. Hariharan and J. A. Pople, *Theor. Chim. Acta,* 1973, **28**, 213; (b) G. A. Petersson and M. A. Al-Laham, *J. Chem. Phys.,* 1991, **94**, 6081; (c) G. A. Petersson, A. Bennett, T. G. Tensfeldt, M. A. Al-Laham, W. A. Shirley and J. Mantzaris, *J. Chem. Phys.,* 1988, **89**, 2193.

55. S. Portmann and H. P. Luthi, *CHIMIA,* 2000, **54**, 766.

56. (a) A. D. Becke, *Phys. Rev. A,* 1988, **38**, 3098; (b) J. P. Perdew and W. Yue, *Phys. Rev. B,* 1986, **33**, 8800.

57. (a) S. Grimme, *J. Comput. Chem.*, 2006, **27**, 1787; (b) A. D. Becke, *J. Chem. Phys.,* 1997, **107**, 8554; (c) J. D. Chai and M. Head-Gordon, *Phys. Chem. Chem. Phys.,* 2008, **10**, 6615; (d) Q. Wu and W. T. Yang, *J. Chem. Phys.,* 2002, **116**, 515.

58. (a) Y. Zhao and D. G. Truhlar, *Theor. Chem. Acc.,* 2008, **120**, 215; (b) Y. Zhao and D. G. Truhlar, *Acc. Chem. Res.,* 2008, **41**, 157.

59. (a) D. Andrae, U. Häussermann, Dolg, M.; H. Stoll and H. Preuss, *Theor. Chim. Acta,* 1990, **77**, 123; (b) A. Bergner, M. Dolg, W. Küchle, H. Stoll and H. Preuss, *Mol. Phys.,* 1993, **80**, 1431.